Delineation of the Alteration Zones by C-N Fractal Model on ASTER Images

Seyyed Saeed Ghannadpour[1*], Samane Esmaelzade Kalkhoran[1], Maedeh Behifar[2], and Hadi Jalili[2]

1. Department of Mining Engineering, Amirkabir University of Technology, Tehran, Iran
2. Iranian Space Research Center, Tehran, Iran

Article Info	Abstract
  Keywords 	In this study, with the aim of identifying alteration zones related to the porphyry copper system, satellite images are processed in study area (the Zafarghand exploration area) in the NE of Isfahan. For this purpose, one of the common methods of separating geochemical anomalies from the background, i.e. fractal Concentration-Number (C-N) model, has been employed. The C-N fractal model will normally be implemented on geochemical samples. While in this study, the digital number values belonging to the pixels of the ASTER sensor image are considered as a systematic sample network and also as input for this model. The output of this processing has been prepared in the form of maps of promising areas of the Zafarghand region. The correspondence of the resulting maps with the alteration map of the region shows that applying the proposed method in determining the propylitic and phyllic alteration zones has had acceptable performance. Finally, with the help of the aforementioned proposed method, a map of the promising areas of the study area has been prepared, and based on that, new zones of alterations have been introduced in the region.

1. Introduction

In recent years, Remote Sensing (RS) and geochemical studies have shown their ability to detect deposits in the early stages, especially in their hidden types. These studies are used in various stages of exploration of mineral deposits, especially in the early stages (General exploration stage), and become more critical for deposits that leave relatively large halos compared to the mass of the deposit [1]. Various methods are used for separating and identifying anomalous areas from the background exist, ranging from non-structural to structural techniques [1]. RS acquires and interprets data about the Earth's surface without direct contact, offering valuable insights for numerous applications, including geological mapping [2-4]. In numerous studies, the application of structural methods for anomaly separation from the background, such as the U spatial statistic method, fractal geometry in various

fractal models, and the singularity method, could be observed [1, 5-9]. This study focuses on combining one of the anomaly separation methods (the concentration-number fractal model) for geochemical anomaly detection with standard RS methods to process ASTER satellite images for the Zafarghand exploration zone.

Fractal geometry is widely used to estimate thresholds and effectively separate anomalous communities. By analyzing the changes in the FD (fractal dimension), anomalous patterns could be identified and distinguished (The fractal dimension is defined as a central value in the domain of nonlinear dynamics and it could be estimated by employing several diverse numerical techniques). In areas where only the background community exists and anomalous values are not observed in the investigated variable (geochemical samples), the distribution diagram for that variable will show

✉ Corresponding author: s.ghannadpour@aut.ac.ir (S.S. Ghannadpour)

minimal fluctuations. Consequently, the FD value will be approximately 2. When the variable surpasses the normal range and enters the realm of anomalies, the presence of pronounced peaks in its variability leads to an increase in the FD value, proportional to the magnitude of the anomaly. This allows for the differentiation between background and anomalous values by comparing their FDs.

Several studies have examined various algorithms and methods for calculating the FD [10-27]. These include variogram analysis, the N-S (Number-Size) model, the C-A (Concentration-Area) model, the C-V (Concentration-Volume) model, the C-P (Concentration-Perimeter) model, the C-N (Concentration-Number) model, the models of U-A and U-N and also the P-A (power spectrum-area) fractal model [10-27].

This research aims to investigate and introduce a proposed method based on the combination of the C-N fractal model (as a method of separating geochemical anomalies) with the band ratio technique (as one of the highlighting methods in remote sensing) will identify the alterations of the Zafarghand exploration area. In this framework, and particularly in the integration of remote sensing and fractal techniques, many studies have been undertaken [28-30].

Considering the significance of this deposit and the need for more in-depth investigations, the present research seeks to detect surface geochemical anomalies in the area using ASTER sensor satellite images. the fractal C-N model, known for its effectiveness and efficiency in geochemical anomaly separation [12, 18, 26, 27], will be applied for processing the satellite imagery.

2. Study area

The Tethys Metallogenic Belt, stretching from Eastern Europe to the Middle East, passes through Iran, which encompasses significant segments of this 1700 km belt and hosts major porphyry copper deposits such as Sarcheshmeh, Miduk, Dalli, Kahang, Zefreh etc [31]. A portion of the belt includes the magmatic arc of Urmia-Dokhtar that the study area is centrally situated within this arc (Figure 1). Early exploration activities in this region comprised geological mapping at a 1:5000 scale, rock sampling, and geophysical surveys. After that, many researches and studies have been done in this area. For example, Sadeghian and Ghafari investigated and studied the petrogenesis of the Zafarghand granitoid mass [32]. Aminoroayaei Yamini et al., with a view to mineralogical and geochemical developments of

the region, investigated the hydrothermal alteration of this deposit [33]. Alaminia et al. conducted geochemical, geophysical, and fluid inclusion studies [32]. Mohammadi et al., through RS studies, investigated the correlation between alteration zones, mineralization and tectonic structures [34]. The porphyry copper of Zafarghand underwent stable isotope and chemistry studies to examine the physicochemical parameters of mineralization and related alteration, with a focus on biotite chloritization [35].

Figure 1. The study area location in the magmatic arc of Urmia-Dokhtar.

The Zafarghand copper exploration area, situated southeast of Ardestan and 110 km northeast of Isfahan in central Iran. The coordinates for this deposit range from 52°23'55" to 52°26'30" E longitude and 33°10'30" to 33°11'52" N latitude (Figure 2) [10]. The rock units of the region could be seen in Figure 2.

In study area of the Zafarghand, a total of 251 samples were collected to conduct a comprehensive geochemical analysis. These samples include:

Soil Samples (67 samples): These samples were taken from various depths and locations within the study area to assess the geochemical anomalies present in the soil.

Rock Samples (184 samples): The lithological collected samples include various lithologies such as quartz diorite, diorite, micro diorite, rhyodacite and dacite.

To facilitate a clearer understanding, the samples in Figure 4 have been differentiated based on their type, providing a visual representation of the distribution and variety of samples collected in the study area.

3. Alteration and mineralization

Most of the rock units of Zafarghand region have been severely altered under the influence of hydrothermal solutions, and the area of alteration that has been created covers an area of about 7 km², part of which is covered by sediments. A distant view of the alterations of the area could be seen in Figure 3 [37].

According to the investigation of samples mentioned above and field observation, this area exhibits various types of alteration, including iron oxide, clay, propylitic, argillic, phyllic and potassic alterations (Figure 4). Some field images of these alterations could be seen in Figures 5, 6 and 7 [37].
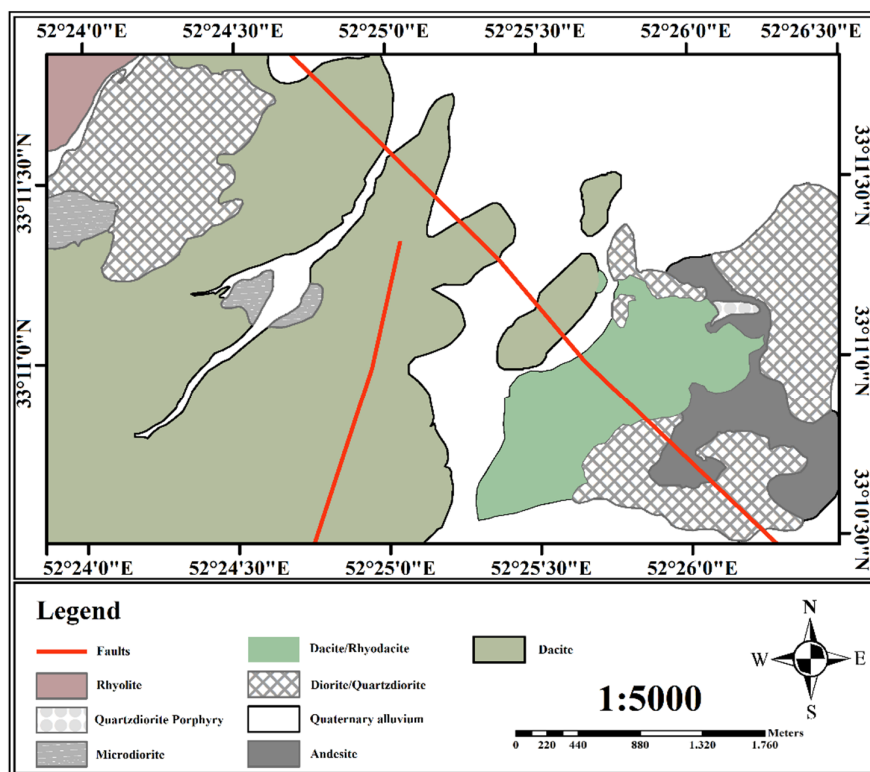

Figure 2. The Zafarghand area geological Map (modified after [31]).

Figure 3. A section of alteration outcrops in the Zafarghand exploration region [37].
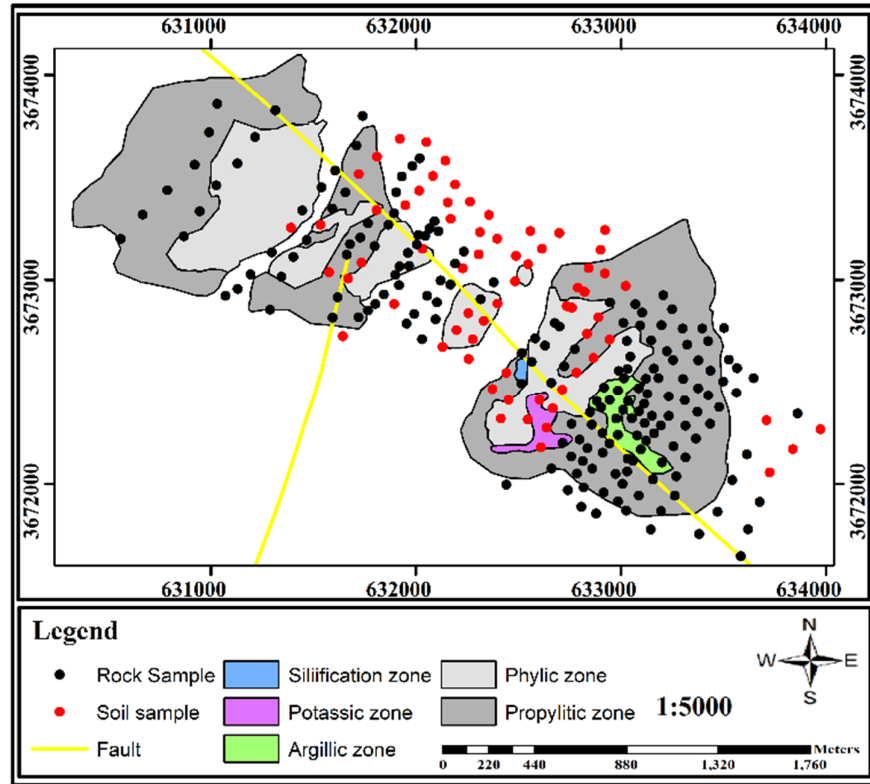
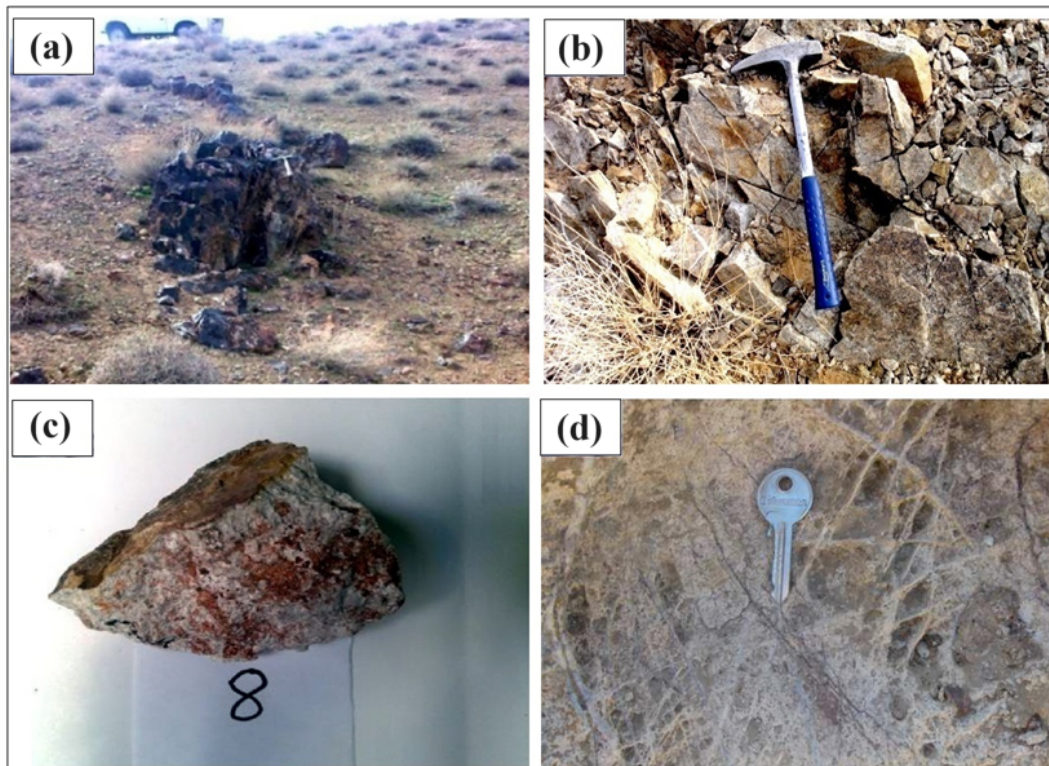**Figure 4. Extension of alteration halos in Zafarghand exploration area.**

Figure 5. Field images of alterations in the study area [37]. (a) Siliceous veins containing copper mineralization in granodiorite rocks with intense potassic alteration (distant view), (b) Diorite rocks with strong potassic alteration (close view), (c) Hand samples of porphyritic dacites showing intense phyllic alteration, and (d) Hematite-quartz stockworks in phyllic alteration in the southern area of Zafarghand.
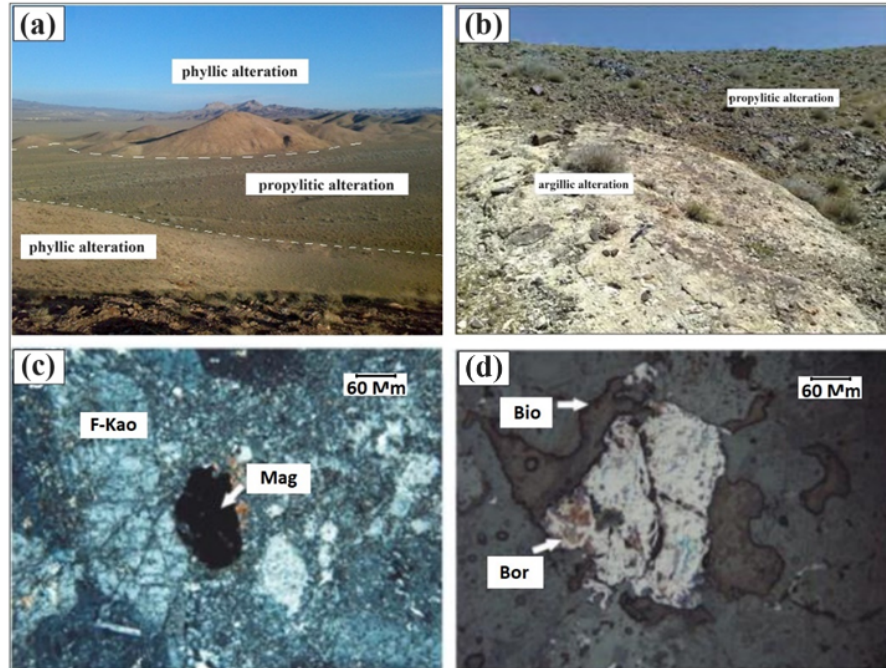
Figure 6. Microscopic and field images of rocks from the Zafarghand exploration area [37]. (a) Outcrop of phyllic and propylitic alteration, (b) Outcrop of argillic and propylitic alteration, (c) Microscopic image of argillic zone dacites in polarized light, and (d) Microscopic image in reflected light corresponding to the conversion of biotite to copper sulfide in the propylitic zone. (F-Kao: Feldspar altered to kaolinite, Mag: Magnetite, Bio: Biotite and Bor: Bornite).
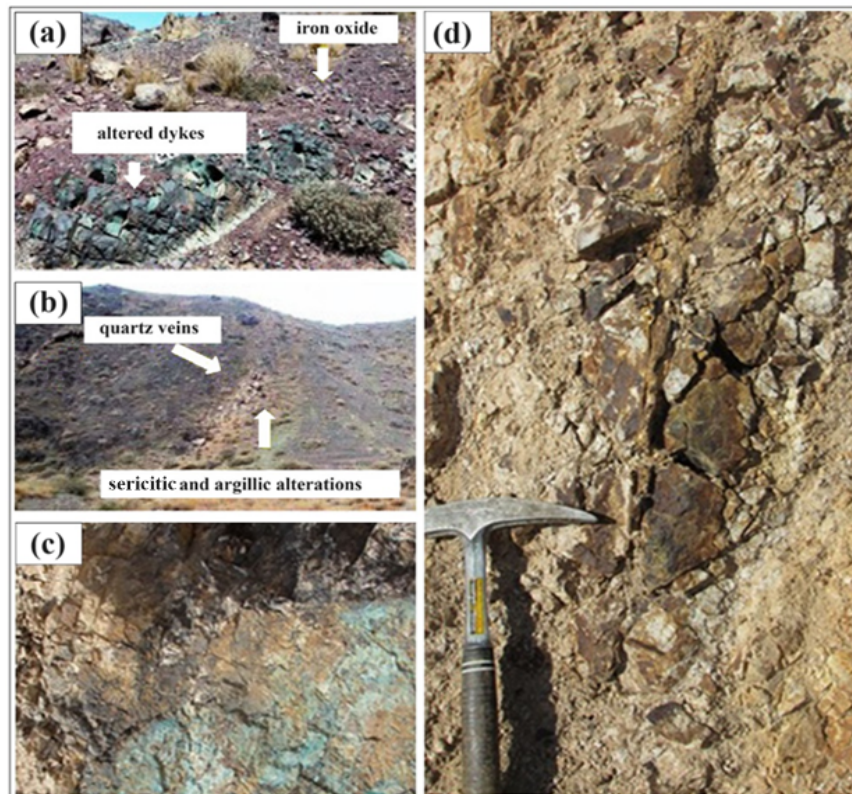

Figure 7. (a) Representation of zones with secondary iron oxides in copper mineralization areas [37], (b) Siliceous veins and their surrounding alterations [37], and (c) & (d) Close-up view of quartz-magnetite veins and stockworks displaying malachite mineralization and iron oxide/hydroxide [37].

4. Material and Method
4.1. Data collection

ASTER satellite images will be employed in this research in order to highlight different alterations.

The ASTER sensor, with its 14 bands provides valuable information about the Earth's surface. It could be employed with other RS satellites to produce more accurate maps. The combining and comparing the Landsat and ASTER data is the most prominent example of such a use [36, 37].

4.2. Pre-processing methods
Log Residual

The log residual method operates by dividing the spectrum of each individual pixel by the spatial and the spectral geometric means that cause a pseudo reflectance data set. To apply this functionality, the hyperspectral imaging library in the image processing toolbox is required.

IARR

The Internal Average Relative Reflectance (IARR) method employs the mean radiance spectrum of the scene, completely. In the next step, it calculates the ratio of this mean spectrum with the spectrum of each individual pixel (all pixel spectra). The underlying assumption is that the mean spectrum represents the solar irradiation spectrum.

Quick Atmospheric Correction

Quick Atmospheric Correction (QUAC) is an empirical atmospheric correction algorithm that operates rapidly. In fact, for correcting hyperspectral and multispectral imagery, it leverages in-scene information. Employing QUAC doesn't require any knowledge of sensor metadata and also doesn't need the sensor to be radiometrically calibrated. Additionally, it supports automated batch processing.

4.3. Band Ratio Enhancement

Employing the Band Ratio (BR) approach is among the widely adopted techniques in satellite imagery processing. This method enables the amplification of spectral disparities between bands, as well as the mitigation of the impacts stemming from variations in shadow and brightness, which could be attributed to topographical factors [38]. By comprehending the spectral attributes of phenomena, as delineated by the spectral signatures of them, diverse phenomena, including anomalies and lithological unit boundaries, could be accentuated through the utilization of this method [39-41].

This technique, by placing a band that has a high reflection (the numerator) divided by a band that has a high absorption (the denominator), makes the difference between this reflection and absorption reach the maximum value. As a result, the brightness value of the pixel corresponding to the target increases (compared to the pixels that do not have the desired target). Since zones containing phyllic alteration have maximum reflectance in the seventh band and maximum absorption in sixth band, band ratio (band 7 / band 6) has been used for enhancement of phyllic alterations, and to highlight zones containing propylitic alteration, the band ratio of (band 6 + band 9) / (band 7 + band 8) has been utilized according to the absorption characteristics in seventh and eighth bands and the reflectance characteristics of the sixth and ninth bands [42-45].

4.4. C-N Fractal Model

The Concentration-Number fractal method (C-N) belongs to the N-S (Number-Size) fractal models [14]. The N-S model could be employed to determine the situation of geological distribution without geostatistical data analysis. In this model, there is a dependency between the required features and the samples' cumulative number. In this research, the C-N model is considered to separate the anomalous values. This model relies on the inverse correlation between concentration and the cumulative frequency of each concentration, particularly larger concentrations. The model is introduced through the equation below [26, 27].

$$N(\geq \rho) \propto \rho^{-\beta} \qquad (1)$$

where ρ represents the chemical concentration of the elements under study, and $N(\geq\rho)$ denotes the total number of samples with concentrations equal to or exceeding ρ. β also corresponds to the FD of the element's distribution.

In the next section (results and discussion), after preprocessing the ASTER satellite images as data preparation, in order to highlight the target, the BR technique will be used. Finally, considering pixels coordinate, the C-N model algorithm is applied to the pixel's DN. The steps are illustrated in Figure 8 in the form of a flowchart.
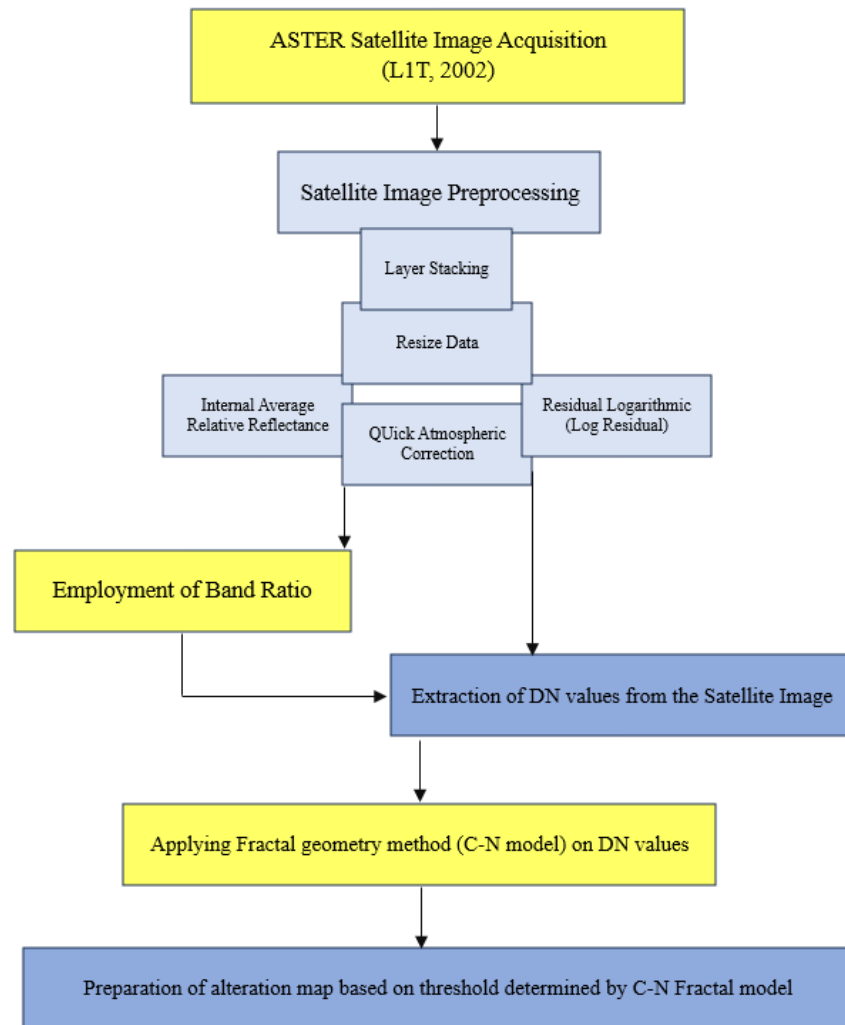
Figure 8. Arrangement of methods applied in image processing.

5. Results and discussion
5.1. Preprocessing of satellite images

The preprocessing techniques are discussed before employing the anomaly separation method, in this section. The radiometric and geometric corrections (as preprocessing operations) are necessary before using the satellite images to obtain their information. For georeferencing the image, geometric corrections are employed, while radiometric corrections address issues such as gases like oxygen and nitrogen, suspended particles in the atmosphere and sunlight passing through clouds that cause interference.

In this study, according to the nature of considered data (Aster satellite images), three pre-processing methods, IARR, Log Residual, and QUAC have been employed [28-30].

5.2. Preparing satellite images for data extraction

To apply the C-N fractal model algorithm, at first, the satellite image was resized based on the presented geographic location in section 2, and then, bands 6, 7, 8 and 9 were considered to extract the values of DN. Considering the bands were according to studies carried out on the porphyry Cu deposits by ASTER sensor (see section 4.3). The mentioned bands are regarded as the most significant bands for highlighting the alterations of porphyry Cu deposits due to their reflectance and absorption characteristics, especially about the desired alterations (phyllic and propylitic) [42-53]. Figure 9 shows the resized output (about these bands).
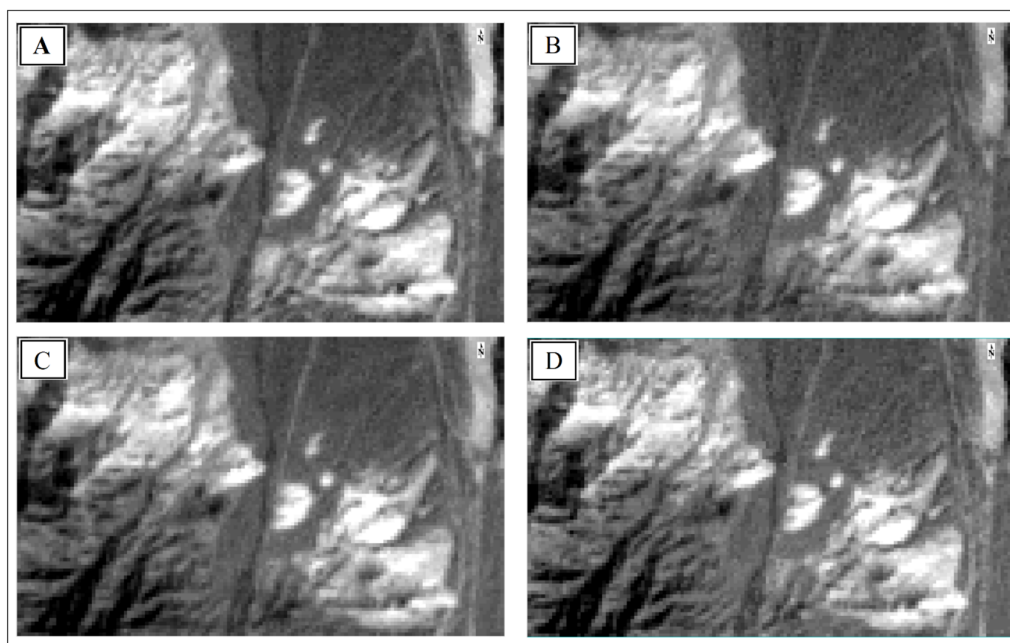
Figure 9. A resized image of the ASTER sensor (SWIR range). A: Sixth band, B: Seventh band, C: Eighth band, and D: Ninth band (the highest and lowest DN are respectively assigned to extreme white and black and the other values include different tons of gray).

Table 1 and Figure 10 show the essential statistical characteristics of DN for desired bands and their histogram, respectively.

In Figure 10, it could be seen that the values of DN exhibit a distribution of normal. Therefore, using anomaly separation methods that typically assume normally distributed data presents no limitations.

5.3. Preparation of alteration map based on Band ratio technique and C-N fractal model

In this part, to prepare the alteration map of the studied area, firstly, the combination of the band's ratio introduced in section 4.3 (Based on the band's ratio reported in Table 2), will be employed to determine the alterations related to hydrothermal mineralization with a special look at porphyry copper deposits [47-49].

The basic statistical characteristics of DN related to the mentioned band ratios along with the histogram of them could be seen in Table 3 and Figure 11, respectively.

Table 1. Statistical characteristics of bands 6 to 9 corresponding to DN values.

Band	Average	Variance	Standard deviation
6	1.6378	0.0551	0.2348
7	1.4454	0.0256	0.1601
8	1.4314	0.0279	0.1671
9	1.4126	0.0219	0.1481

Table 2. Band ratios used to determine alterations (porphyry copper).

No.	Alteration type	Band ratio
1	Propylitic	(band 6 + band9) / (band 7 + band 8)
2	Phyllic	(band 7 / band 8)

Table 3. Statistical characteristics of DN values related to the band ratios in Table 2.

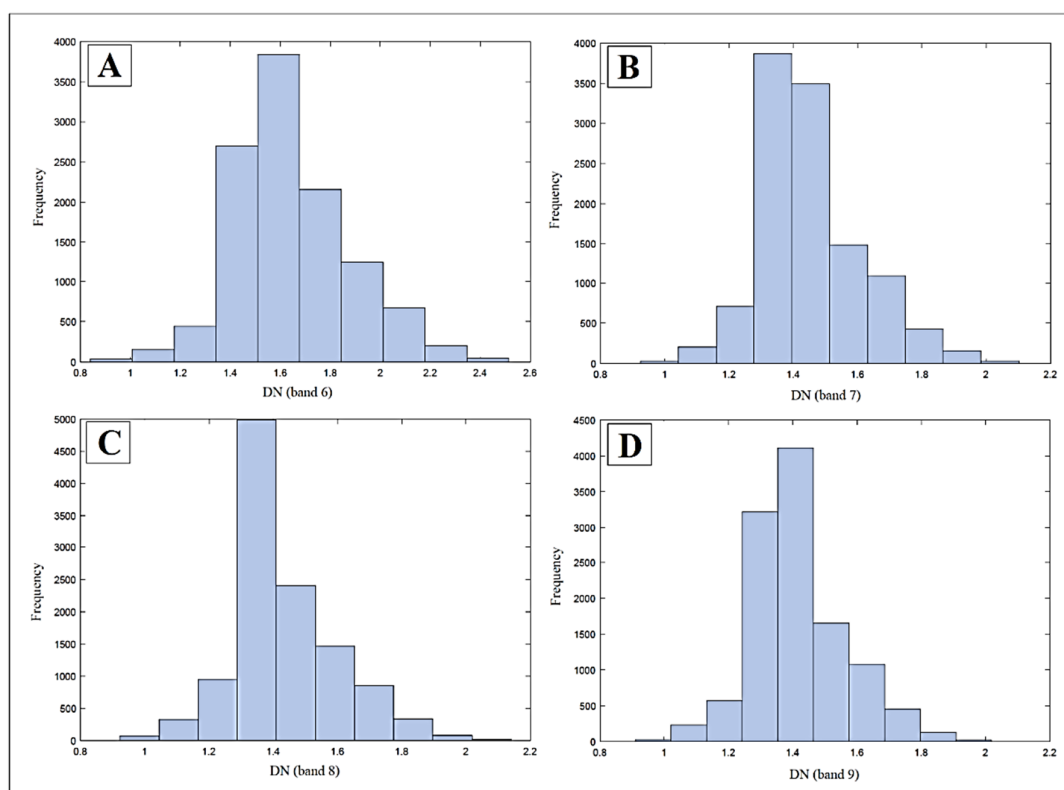| No.	Alteration Type	Average	Variance	Standard deviation
1	Propylitic	1.0594	0.0011	0.0333
2	Phyllic	0.8874	0.0021	0.0457

Figure 10. The frequency diagram of DN value. A: Sixth band, B: Seventh band, C: Eighth band, and D: Ninth band.
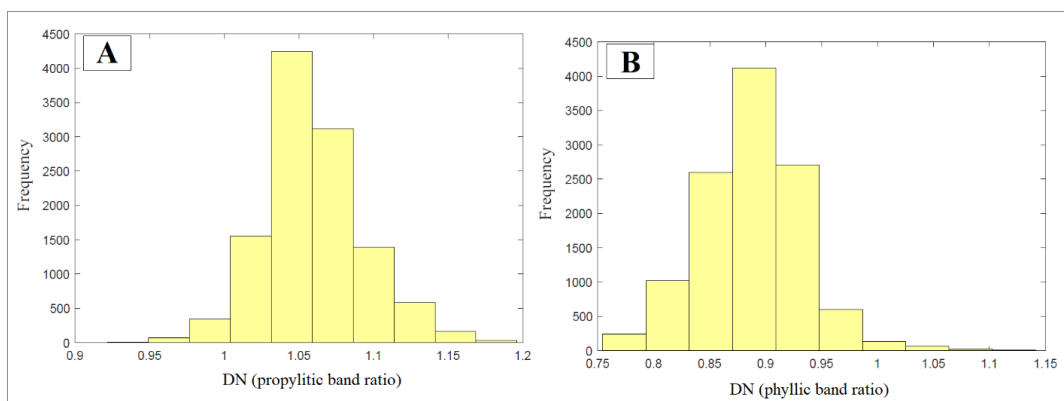

Figure 11. Histogram of the calculated DN value for the band ratios reported in Table 2, propylitic (A), and phyllic (B).

In Figure 11, it could be seen that the distribution of DN values related to the band ratios (in order to highlight the mineralization alterations of the studied area) also follows the normal distribution and there is no need to normalize the data. Therefore, in the next step, a fractal model of C-N could be employed to detect the threshold.

Choosing the C-N fractal model according to the value of DN to each pixel that represents the reflectance specific to it, seems to have an acceptable performance to separate anomaly. Because satellite images, based on their raster

nature, provide the number of image pixels and the DN specific to it (as the concentration of each pixel) for the concentration-number fractal model.

5.3.1. Applying C-N fractal model algorithm to DN values

The weakness of the C-N fractal model compared to other fractal models is considering the concentration of elements in one point. Whereas, in algorithm of other fractal models, concentration of elements in considered based on a set of points. For example, the Concentration-Area (C-A) model,

each cell refers to a set of points (an area of the concentration density) that is calculated through interpolation methods.

By considering the nature of the investigated data (i.e. pixels of satellite images) and the fact that each pixel belongs to a square area with a certain side length (as for the SWIR of ASTER sensor in this study, 30 meters), this limitation has significantly been removed.

In order to apply the C-N fractal model, the DN of band ratios introduced in the previous part, from the SWIR range of the Zafarghand exploration area, are provided as input to the C-N fractal model algorithm. Finally, the full logarithmic diagram of concentration values (DN values of satellite images) will be prepared in relation to the number of pixels in their content (Figure 12).

With a more detailed and technical look at these diagrams (Figure 12), which represent the C-N fractal model, for the models related to the DN values of each band ratio, three breaking points and, in fact, four different populations could be considered (Figure 13). The characteristics of the mentioned populations are also shown in Table 4.

Finally, with the help of Surfer software (SURFER version 11.0 software), the images of the prospective areas of the Zafarghand area have been prepared based on the threshold determined by the fractal method (C-N model) (Figure 14) .
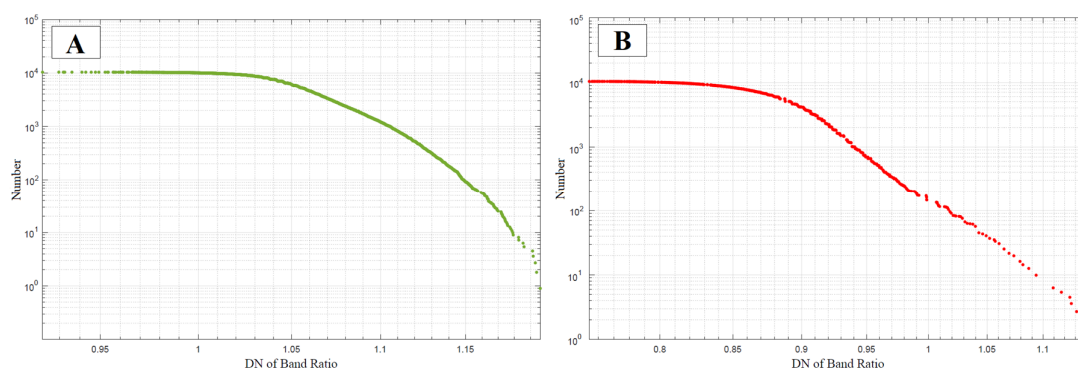

Figure 12. Fractal C-N model for DN values of SWIR range, propylitic band ratio (A), and phyllic band ratio (B).
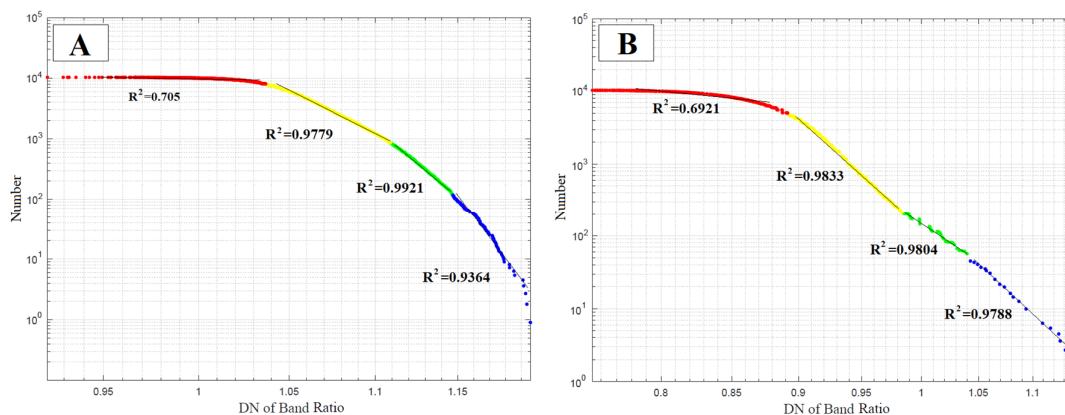

Figure 13. Fitting the lines to the C-N fractal model to show different populations, propylitic band ratio (A), and phyllic band ratio (B).

Table 4. DN value classes related to different populations about propylitic and phyllic alterations.

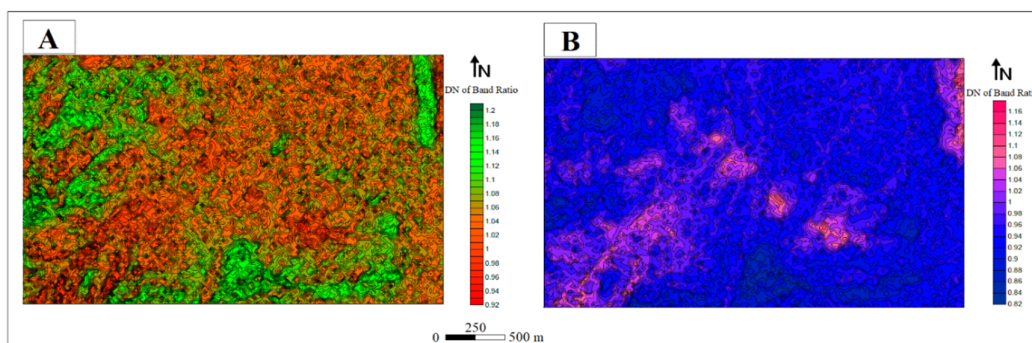| Population	Propylitic alteration	FD (Pro)	Phyllic alteration	FD (Phy)
1	<1.037	0.011	<0.892	0.018
2	1.037-1.109	0.148	0.892-0.985	0.555
3	1.109-1.147	0.541	0.985-1.04	0.641
4	1.147-1.196	1.422	1.04-1.141	1.44

Figure 14. Image of the prospective areas of the Zafarghand district using the C-N fractal method, propylitic band ratio (A) and phyllic, band ratio (B).

As could be seen in Figure 14, the promising zones (anomalous zones) identified by the determination of threshold limits (reported in Table 4) in the C-N fractal method for the band ratio of the bands corresponding to propylitic and phyllic alterations, correspond favorably to the mineralized zones and alterations of Zafarghand exploration area (Figure 4). In more detail, it could be noted that the promising regions in Figure 14-A, which are related to the band ratio associated with the propylitic alteration, have a very good match with the propylitic modifications shown in Figure 4. It should also be noted that the highlighted areas in Figure 14, part B, as DN values related to the band ratio of phyllic alteration, have a very good relationship with the sericitic alteration identified in Figure 4.

In order to better understand this issue, the maps in Figure 14 have been prepared with the alteration map of Figure 4 in the form of an overlapping image (Figure 15).

In this image, the alteration determined based on the band ratios of propylitic and phyllic alteration could be seen in competent compliance with the propylitic and sericite alteration zones in the map of Figure 4.
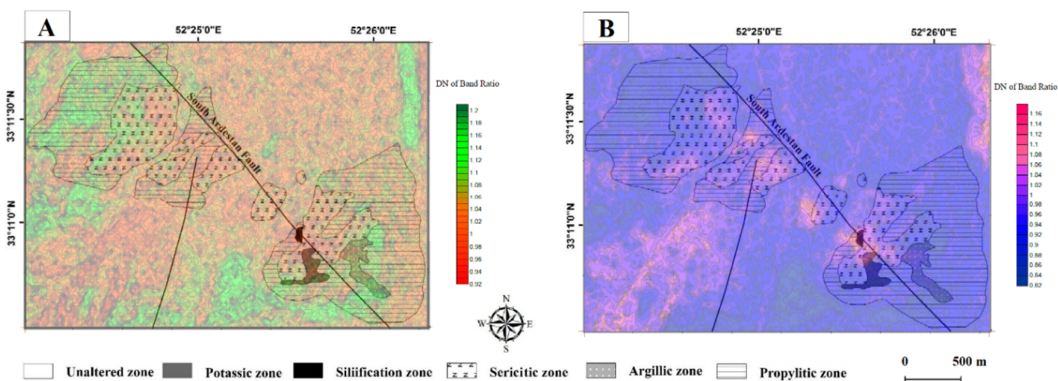

Figure 15. The overlapping image of the Zafarghand promising areas determined by the C-N fractal model with its alteration map, propylitic band ratio (A), and phyllic band ratio (B).

Of course, it is worth noting that the DN values specified in the northeast and especially southwest of the images in parts A and B of Figure 14 (or Figure 15) and their mismatch with Figure 4 are due to the lack of sampling from the northeast and southwest regions of the study area (as in Figure 4, the location of the samples shows this issue). Therefore, according to the preparation of the alteration map of the region (Figure 4) based on this sampling, this mismatch seems logical.

In order to validate the identified areas in the northeast and southwest of Zafarghand region,

field studies have been conducted in these areas, the field observations confirm the existence of such alterations.

Finally, based on the results obtained from the processing of ASTER satellite images by the C-N fractal model and their confirmation by the region's alteration map and field observations, a final map has been prepared as the promising areas of Zafarghand region with the display of propylitic and phyllic alterations and in Figure 16 is shown.
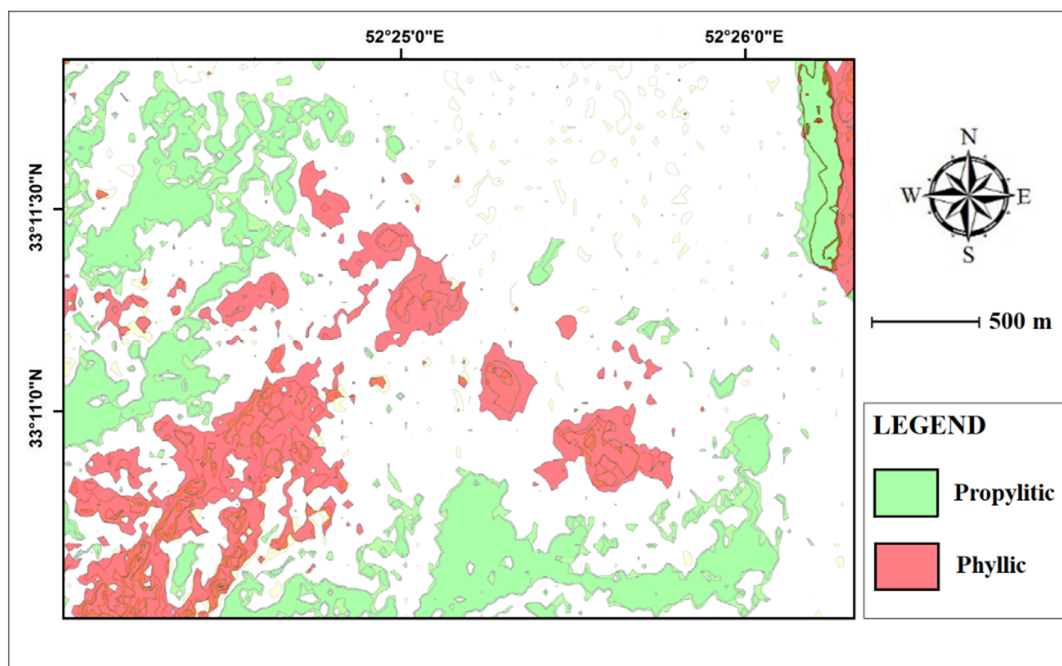
Figure 16. The map of the promising areas determined by the C-N fractal model in the processing of the ASTER sensor images.

6. Conclusions

In this research, by using the concept of satellite image processing, the satellite images of ASTER sensors were investigated and studied. For this purpose, at first, with the help of the band ratio technique, the DN of each pixel in the satellite image of exploration area of the Zafarghand (in the NE of Isfahan) was calculated. Then, the C-N fractal model was used to the DN values in order to separate the anomalies related to the alterations of the region. In the next step, the promising areas map was prepared and compared with the alteration map of the Zafarghand exploration area. The results showed the successful performance of this proposed method (combined technique) in processing raster-based satellite images, because the promising areas determined by this method are very well related to the propylitic and phyllic alterations. Finally, the promising areas were prepared in the form of a map as output. It should also be mentioned that because in satellite images, the DN of each pixel is representative of a square area with a certain side length, the C-N fractal model could be considered equivalent to the C-A fractal model and accordingly the breaking points of these two models are also equal to each other.

References

[1]. Hezarkhani, A., & Ghannadpour, S.S. (2015). Exploration Information Analysis. Amirkabir University of Technology Publications.

[2]. Biranvandpour, A., & Hashim, M. (2014). ASTER, ALI and Hyperion sensors data for lithological mapping and ore minerals exploration. *Springer Plus, 3*, 130.

[3]. Ghassemian, H. (2016). A review of remote sensing image fusion methods. *Information Fusion*, *32*, 75–89. Elsevier B.V.

[4]. Van der Meer, F., Hecker, C., van Ruitenbeek, F., van der Werff, H., de Wijkerslooth, C., & Wechsler, C. (2014). Geologic remote sensing for geothermal exploration: A review. *International Journal of Applied Earth Observation and Geoinformation, 33(1),* 255–269.

[5]. Cheng, Q, Agterberg, F.P., & Bonham-Carter, G.F. (1996). A spatial analysis method for geochemical anomaly separation. *Journal of Geochemical Exploration*, *56*, 183–I95.

[6]. Cheng, Q., Yaguang, X., & Eric, G. (2000). Integrated spatial and spectrum method for geochemical anomaly separation. *Natural Resources Research, 9(1),* 43–52.

[7]. Ghannadpour, S.S., & Hezarkhani, A. (2016). Introducing 3D U-statistic method for separating anomaly from background in exploration geochemical data with associated software development. *Journal of Earth System Science, 125(2),* 387–401.

[8]. Ghannadpour, S.S., & Hezarkhani, A. (2016). Exploration geochemistry data-application for anomaly separation based on discriminant function analysis in the

Parkam porphyry system (Iran). *Geoscience Journal, 20(6),* 837–850.

[9]. Ghannadpour, S.S., Hezarkhani, A., & Sharifzadeh, M. (2017). A method for extracting anomaly map of Au and As using combination of U-statistic and Euclidean distance methods in Susanvar district, Iran. *Journal of Central South University, 24,* 2693-2704.

[10]. Ghannadpour, S.S., & Hezarkhani, A. (2017). Comparing U-statistic and nonstructural methods for separating anomaly and generating geochemical anomaly maps of Cu and Mo in Parkam district, Kerman, Iran. *Carbonates and Evaporites, 32(2),* 155–166.

[11]. Ghannadpour, S.S., Hezarkhani, A., & Roodpeyma, T. (2017). Combination of Separation Methods and Data Mining Techniques for Prediction of Anomalous Areas in Susanvar, Central Iran. *African Journal of Earth Sciences, 134,* 516–525.

[12]. Ghannadpour, S.S., & Hezarkhani, A. (2018). Providing the bivariate anomaly map of Cu–Mo and Pb–Zn using combination of statistic methods in Parkam district, Iran. *Carbonates and Evaporites, 33(3),* 403–420.

[10]. B Behbahanı, H Haratı, P Afzal, M Lotfı, 2023. Determination of alteration zones applying fractal

[13]. Zamyad, M., Afzal, P., Pourkermani, M., Nouri, R., & Jafari, M.R. (2019). Determination of hydrothermal alteration zones using remote sensing methods in Tirka Area, Toroud, NE Iran. *Journal of the Indian Society of Remote Sensing, 47,* 1817-1830

[14]. Mandelbrot, B.B. 1983. The fractal geometry of nature. W.H. Freeman and company, San Francisco, New York, 468 p.

[15]. Cheng, Q., Agterberg, F.P., & Ballantyne, S.B. (1994). The separation of geochemical anomalies from background by fractal methods. *Journal of Geochemical Exploration, 51,* 109- 130.

[16]. Li, C., Ma, T., & Shi, J. (2003). Application of a fractal method relating concentrations and distances for separation of geochemical anomalies from background. *Journal of Geochemical Exploration, 77,* 167-175.

[17]. Afzal, P., Alghalandis, Y. F., Khakzad, A., Moarefvand, P., & Omran, N.R. (2011). Delineation of mineralization zones in porphyry Cu deposits by fractal concentration–volume modeling. *Journal of Geochemical exploration, 108 (3)*, 220-232.

[18]. Hassanpour, S., & Afzal, P. (2013). Application of concentration–number (C-N) multifractal modeling for geochemical anomaly separation in Haftcheshmeh porphyry system, NW Iran. *Arabian Journal of Geosciences, 6,* 957-970.

[19]. Nazarpour, A., Omran, N.R., & Paydar, G.R. (2015). Application of multifractal models to identify geochemical anomalies in Zarshuran Au deposit, NW Iran. *Arabian Journal of Geosciences, 8,* 877-889.

[20]. Momeni, S., Shahrokhi, S.V., Afzal, P., Sadeghi, B., Farhadinejad, T., & Nikzad, M.R. (2016). "Delineation of the Cr mineralization based on the stream sediment data

utilizing fractal modeling and factor analysis in the Khoy 1:100,000 sheet, NW Iran. *Bulletin of the Mineral Research and Exploration, 152,* 1-17.

[21]. Ahmadfaraj, M., Mirmohammadi, M., & Afzal, P. (2016). Application of fractal modeling and PCA method for hydrothermal alteration mapping in the Saveh area (Central Iran) based on ASTER multispectral data. *International Journal of Mining and Geo-Engineering, 50(1),* 37-48.

[22]. Afzal, P., Ahmadi, K., & Rahbar, K. (2017). Application of fractal-wavelet analysis for separation of geochemical anomalies. *African Journal of Earth Science, 128,* 27-36.

[23]. Koohzadi, F., Afzal, P., Jahani, D., & Pourkermani, M., (2021). Geochemical exploration for Li in regional scale utilizing Staged Factor Analysis (SFA) and Spectrum-Area (S-A) fractal model in north central Iran. *Iranian Journal of Earth Sciences, 13,* 299-307.

[24]. Shahbazi, S., Ghaderi, M., & Afzal, P. (2021). Prognosis of gold mineralization phases by multifractal modeling in the Zehabad epithermal deposit, NW Iran. *Iranian Journal of Earth Sciences, 13,* 31-40.

[25]. Farhadi, S., Afzal, P., Boveiri Konari, M., Daneshvar Saein, L., & Sadeghi, B. (2022). Combination of Machine Learning Algorithms with Concentration-Area Fractal Method for Soil Geochemical Anomaly Detection in Sediment-Hosted Irankuh Pb-Zn Deposit, Central Iran. *Minerals, 12(6),* 689.

[26]. Ghannadpour, S.S., & Hezarkhani, A. (2022). A new method for determining geochemical anomalies: UN and UA fractal models. *International Journal of Mining & Geo-Engineering, 56(2),* 181-190.

[27]. Ghannadpour, S.S., & Hezarkhani, A. (2022). Delineation of geochemical anomalies for mineral exploration using combining U-statistic method and fractal technique: UN and UA models. *Applied Earth Science, 131(1),* 32-40.

[28]. Ghannadpour, S.S., Hasiri, M., Talebiesfandarani, S., & Jalili, H. (2024). Applying the fractal geometry method (C-A model) to Processing ASTER satellite images. *Journal of Mineral Resources Engineering, 9(3),* 10.30479/jmre.2024.19329.1665. (In Persian with English Abstract). https://jmre.journals.ikiu.ac.ir/article_3314.html

[29]. Ghannadpour, S.S., Hasiri, M., Jalili, H., & Talebiesfandarani, S. (2024). Satellite Image Processing: Application for Alteration Separation based on U-Statistic Method in Zafarghand Porphyry System (Iran). *Journal of Mining and Environment, 15(2),* 667-681.

[30]. Ghannadpour, S.S., Esmailzadeh Kalkhoran, S., Jalili, H., & Behifar, M. (2024). Delineation of mineral potential zone using U-statistic method in processing satellite remote sensing images. *International Journal of Mining and Geo-Engineering, 57(4),* 445-453.

[31]. Alaminia, A., Bagheri, H., & Salehi, M. (2017). Geochemical and geophysical investigations, and fluid inclusion studies in the exploration area of Zafarghand (Northeast Isfahan, Iran). *Journal of Economic Geology, 9*(2), 295-312. (In Persian with English Abstract)

[32]. Sadeghian, M., & Ghafari, M. (2011). Petrogenesis of the Zafarghand Granitoid Massif (Southeast of Isfahan). *Petrology, 2(6),* 47-70.

[33]. Aminoroayaei Yamini, M., Tutti, F., & Ahmadian, J. (2016). Hydrothermal Alteration of Porphyry Copper Deposit in the Southwest of Zafarghand with Emphasis on Mineralogical and Geochemical Changes in the Area. *Journal of Earth Sciences Research*, *7(25),* 75-90.

[34]. Mohammadi, S., Nedaei, A.R., & Aalami Nia, Z. (2018). Analysis of the relationship between mineralization and alteration zones with tectonic structures using remote sensing studies in south Ardestan area (northeastern Isfahan). *Geotectonics, 7,* 29-47.

[35]. Aminoroayaei Yamini, M., Tutti, F., Haschke, M., Ahmadian, j., & Murata, M. (2016). Synorogenic copper mineralization during the Alpine–Himalayan orogeny in the Zafarghand copper exploration district, Central Iran: petrography, geochemistry and alteration thermometry. *Geological Journal, 25(2),* 263-281.

[36]. Esmailzadeh Kalkhoran, S., Ghannadpour, S.S., Moeini Rad, A., & Jalili, H. (2024). comparing the Performance of ASTER and LANDSAT 8 Satellite Images in Identifying Iron Oxide and Porphyry Copper Alterations in Zafarghand Region of Isfahan Province. *Journal of Mineral Resources Engineering, 9(1),* 41-65.

[37]. Esmailzadeh Kalkhoran, S., Ghannadpour, S.S., Jalili, H., & Moeini Rad, A. (2024). Investigating porphyry copper alterations and spectral behavior of related minerals using ASTER satellite images in the Zafarghand region, Isfahan. *Advanced Applied Geology, Articles in Press:* 10.22055/aag.2024.45697.2425 (In Persian with English Abstract). https://aag.scu.ac.ir/article_19164.html

[38]. Hewson, R.D., Cudahy, T.J., Mizuhiko, S., Ueda, K., & Mauger, A.j. (2005). Seamless geological map generation using ASTER in the Broken Hill-Curnamona province of Australia. *Remote Sensing of Environment, 99*, 159-172.

[39]. Ghrefat, H., Awawdeh, M., Howari, F., & Al-Rawabdeh, A. (2023). Mineral exploration using multispectral and hyperspectral remote sensing data. *Geoinformatics for Geosciences,* 197–222.

[40]. Pournamdari, M., Hashim, M. & Pour, A. B. (2014). Spectral transformation of ASTER and Landsat TM bands for lithological mapping of Soghan ophiolite complex, south Iran. *Advances in Space Research, 54(4)*, 694-709.

[41]. Azizi, A., Tarverdi, M. A., & Akbarpour, A. (2010). Extraction of hydrothermal alterations from ASTER SWIR data from east Zanjan, northern Iran. *Advances in Space Research, 54(4)*, 99-109.

[42]. Grove, C.I., Hook, S.J. & Paylor III, E.D. (1992). Laboratory reflectance spectra of 160 minerals, 0.4 to 2.5 micrometers.

[43]. Hunt, G.R. & Salisbury, J.W. (1971). Visible and near infrared spectra of minerals and rocks. II. Carbonates. *Modern Geology, 2,* 23-30.

[44]. Salisbury, J.W. & D'Aria, D.M. (1992). Emissivity of terrestrial materials in the 8–14 μm atmospheric window. *Remote Sensing of Environment, 42(2),* 83-106.

[45]. Vicente, L.E. & de Souza Filho, C.R. (2011). Identification of mineral components in tropical soils using reflectance spectroscopy and advanced spaceborne thermal emission and reflection radiometer (ASTER) data. *Remote Sensing of Environment, 115*(8), 1824-1836.

[46]. Beiranvand Pour, A., & Hashim, M. (2011). Identification of hydrothermal alteration mineral for exploration of porphyry copper deposit using ASTER data, SE Iran. ELSEVER: *Journal of Asian Earth Sciences, 42*, 1309-1323.

[47]. El-Qassas, R.A.Y., Abu-Donia, A.M., & Omar, A.E.A. (2023). Delineation of hydrothermal alteration zones associated with mineral deposits, using remote sensing and airborne geophysics data. A case study: El-Bakriya area, Central Eastern Desert, Egypt. *Acta Geodaetica et Geophysica, 5,* 71–107.

[48]. Shahi, H., & Kamkar-Rouhami, A. (2014). A GIS-based weights of evidence model for mineral potential mapping of hydrothermal gold deposits in Torbat-e-Heydarieh area. *Journal of Mining and Environment, 5(2),* 79-89.

[49]. Mhangara, P. (2005). Testing the ability of ASTER (Advanced spaceborne thermal emission and reflection radiometer) to tap hydrothermal alteration zones: a case study of the Haib Porphyry Copper-Molybdenum Deposit, Namibia. MSc dissertation, *Stellenbosch University*.

[50]. Pour, A.B., & Hashim, M. (2012). The application of ASTER remote sensing to porphyry copper and epithermal gold deposits. *Ore Geology Reviews, 44,* 1-9.

[51]. Nouri, R., Jafari, M. R., Arain, M., & Feizi, F. (2012). Hydrothermal Alteration Zones Identification Based on Remote Sensing Data in the Mahin Area, West of Qazvin Province, Iran. *In Proceedings of World Academy of Science, Engineering and Technology 67, World Academy of Science, Engineering and Technology.*

[52]. Sadek, M.F., Ali-Bik, M.W., & Hassan, S.M. (2015). Late Neoproterozoic basement rocks of Kadabora-Suwayqat area, Central Eastern Desert, Egypt: geochemical and remote sensing characterization. *Arabian Journal of Geoscience, 8,* 10459–10479.

[53]. Kumar, C., Shetty, A., Raval, S., Sharma, R., & Ray, P. K. C. (2015). Lithological Discrimination and Mapping using ASTER SWIR Data in the Udaipur area of Rajasthan, India. *Procedia Earth Planet. Sci, 11,* 180–188.

ترسیم نواحی تغییر توسط مدل فراکتالی C-N در تصاویر ASTER

سید سعید قنادپور¹*، سمانه اسماعیل‌زاده کلخوران¹، مائده بهی فر² و هادی جلیلی²**

۱. گروه مهندسی معدن، دانشگاه صنعتی امیرکبیر، تهران، ایران

۲. مرکز تحقیقات فضایی ایران، تهران، ایران

٭ نویسنده مسئول مکاتبات: s.ghannadpour@aut.ac.ir

چکیده:

در این مطالعه، با هدف شناسایی زون‌های دگرسانی مرتبط با سیستم مس پورفیری، تصاویر ماهواره‌ای در منطقه مورد مطالعه (منطقه اکتشافی ظفرقند) در شمال شرق اصفهان پردازش شده است. برای این منظور، یکی از روش‌های متداول جداسازی ناهنجاری‌های ژئوشیمیایی از پس‌زمینه، یعنی مدل غلظت-عدد فراکتال (C-N) استفاده شده است. مدل فراکتال C-N به طور معمول بر روی نمونه‌های ژئوشیمیایی اجرا می‌شود.در حالی که در این مطالعه، مقادیر عدد دیجیتال متعلق به پیکسل‌های تصویر حسگر ASTER به عنوان یک شبکه نمونه سیستماتیک و همچنین به عنوان ورودی برای این مدل در نظر گرفته می‌شود. خروجی این پردازش در قالب نقشه مناطق امیدبخش منطقه ظفرقند تهیه شده است. مطابقت نقشه‌های به دست آمده با نقشه دگرسانی منطقه نشان می‌دهد که بکارگیری روش پیشنهادی در تعیین پهنه‌های دگرسانی پروپیلیتی و فیلیک عملکرد قابل قبولی داشته است. در نهایت با استفاده از روش پیشنهادی فوق، نقشه‌ای از نواحی امیدوارکننده منطقه مورد مطالعه تهیه شده و بر این اساس، پهنه‌های دگرسانی جدیدی در منطقه معرفی شده است.

کلمات کلیدی: هندسه فراکتال، مدل C-N، پردازش تصویر، ASTER، ظفرقند.